Local lattice distortions around interstitial oxygen in niobium

P. Barbéris, B. Beuneu, C.-H. de Novion

Classification
Physics Abstracts
61.70B

Local lattice distortions around interstitial oxygen in niobium

P. Barbéris, B. Beuneu and C.-H. de Novion

CEA/CEREM, Laboratoire des Solides Irradiés, Ecole Polytechnique, 91128 Palaiseau, France

(*Received 6 November 1991, accepted in final form 24 December 1991*)

Résumé. — La diffusion diffuse élastique de neutrons dans un cristal $NbO_{0,023}$ a été mesurée dans le plan $[1\bar{1}0]$ du réseau réciproque. Une méthode de déconvolution des spectres a permis d'améliorer les performances d'analyse du temps de vol près des pics de Bragg où la contribution inélastique due aux phonons de faible énergie est importante. On observe une diffusion Huang autour des pics de Bragg, un maximum marqué près de (1,3 1,3 1,3) et un signal diffus cohérent dans tout le plan. Il n'apparaît pas de manifestation claire d'un ordre local entre impuretés. Les premiers voisins des interstitiels d'oxygène sont si fortement repoussés que les développements analytiques habituels sont inutilisables ; les données ont donc été analysées à l'aide d'un modèle simple supposant les défauts isolés et ne considérant que les perturbations sur les quatre premières couches de voisins.

Abstract. — The elastic neutron diffuse scattering has been measured on a quenched $NbO_{0.023}$ single crystal in the $[1\bar{1}0]$ reciprocal plane. Because of the large inelastic contribution due to low-energy phonons, a deconvolution method has been developed which increases the time-of-flight analysis accuracy. The coherent elastic diffuse intensity is composed of a diffuse Huang scattering around the Bragg peaks, a strong maximum near the (1.3 1.3 1.3) position and a coherent diffuse signal in the whole plane. There is no clear evidence for a short-range order between interstitials. The first neighbours of the oxygen interstitials are so strongly repulsed that the usual analytic developments are not justified and the data have been analysed within a simple model assuming that the defects are isolated and considering only the perturbation over the four first neighbouring shells.

1. Introduction.

The lattice distortions induced by light impurities in body-centred cubic Nb have been studied by means of X-ray Huang scattering, Stokes-Wilson scattering and diffuse neutron scattering far from the Bragg peaks [1, 2].

For oxygen (or nitrogen) impurities, some peaks have been observed, similar to those given by the ω phase observed in Nb-Zr alloys. Dosch *et al.* [1] have explored the neighbourhoods of such peaks far away from the origin of the reciprocal space (scattering vector $|q| \approx 8$ Å^{-1}) by means of neutron diffuse scattering. They could explain altogether X-ray Huang scattering, Stokes-Wilson scattering and neutron diffuse scattering around the ω type peaks within the Kanzaki forces model [3] (using three forces). Very high displacements were found on the first atomic shells around the defect (see Tab. I), which were related to the formation of ω phase « embryos ».

On the other hand, de Novion and Just [4] have measured the neutron diffuse scattering in the (001) reciprocal plane around the origin ($0.2\ Å^{-1} \leq |q| \leq 2.25\ Å^{-1}$) for two compositions $NbO_{0.026}$ and $NbO_{0.036}$. Diffuse maxima were found in positions (1/2 1/2 0), (1/2 0 0) and (1 0 0). These peaks could be explained neither by a Kanzaki forces calculation nor by the formation of random oxygen clusters suggested by Gibala *et al.* [5] from internal friction measurements. The oxygen atoms (isolated or in small clusters) were thus supposed to be strongly correlated, at least in the (001) planes (similar ordering of dilute impurities in a b.c.c. host has already been observed in the case of $Ta_{64}C$ [6]). The internal friction results of Weller *et al.* [7] on NbO_x were also attributed to a repulsive long range interaction between interstitials.

As the diffuse intensity is dominated by distortion effects at large $|q|$ values (domain of Dosch *et al.* measurements), and by short-range-order (SRO) effects at low $|q|$ values (de Novion *et al.* measurements), these two sets of experiments cannot be compared. Moreover, these data have been interpreted within the famework of the Kanzaki forces : this model assumes that the force constants between the Nb atoms are not affected by the presence of the defect. In the NbO_x system where the distortions can reach 0.4 Å, this assumption is certainly not justified.

We have therefore undertaken at the Laboratoire Léon Brillouin ([1]) (Saclay, France) a study of the neutron elastic diffuse scattering in this Nb(O) system, in an intermediate domain in $|q|$ with the double intention of looking for short-range-ordering between interstitials and of measuring the atomic displacements without assumptions on their amplitude.

2. Experiments.

2.1 SAMPLE PREPARATION AND CHARACTERISATION. — A niobium single crystal in the form of a 12.5 mm in length and 6 mm diameter cylinder, with a nominal purity 99.999 % was obtained from Goodfellow Metals Ltd. This sample was oxidized at 1 050 °C in a dynamic pressure of 2×10^{-4} torr of oxygen for 30 hours, then heated at 1 400 °C in a 5×10^{-8} torr vacuum for 60 hours in order to homogenize the oxygen concentration, and quenched in water from 1 000 °C.

A polycrystalline sample of the same shape with a large grain size was submitted to the same treatment in order to check the homogeneity of the oxygen concentration. During the whole process the lattice parameter of the single crystal was increased from 3.2980 Å to 3.3075 (± 0.0010) Å, which leads to a 2.3 ± 0.2 at% oxygen concentration. The microhardness increase, from 96 to about 350 (335 for the polycrystal), corresponds to about 2.7 at% oxygen [8]. This last measurement being more sensitive to surface effects, the oxygen concentration is assumed to be $c = 2.3$ at%.

2.2 DIFFUSE NEUTRON SCATTERING MEASUREMENTS. — These measurements were performed on the two-axis spectrometer G4-4 of the LLB (Saclay, France), described in detail in [9]. Each of the 52 He^3 detectors integrated the intensity in $\delta(2\theta) = 2.5°$. With a wavelength $\lambda = 2.6$ Å, the scattering vector range was $0.4\ Å^{-1} \leq |q| \leq 4.4\ Å^{-1}$. A time-of-flight analysis allowed us to eliminate most of the inelastic scattering. The sample was held at room temperature in a vacuum chamber in order to avoid the background due to scattering by air.

The diffuse scattering has been measured in the $[1\bar{1}0]$ reciprocal plane before and after oxidization of the crystal. Before oxidization the intensity is nearly constant in the reciprocal space and mostly incoherent (6.0 mb). This incoherent cross-section is much higher than that measured in [10] and [4] for pure niobium (< 1 mb). After oxidization, the incoherent signal

([1]) Laboratoire commun CEA-CNRS.

is significantly decreased (≈ 2.4 mb), showing that the impurities (probably hydrogen) have been partly eliminated.

2.3 INTENSITY MAP. — The diffuse scattering iointensity map in the $[1\bar{1}0]$ reciprocal plane for the $NbO_{0.023}$ single crystal at room temperature is given in figure 1a in Laue units (1 Laue $= N \,.\, c \,.\, (1 - c/3) \,.\, b_0^2$ i.e. 7.7 mb per Nb site). The data have been corrected for background and calibrated by comparison with a vanadium standard.

High diffuse scattering intensities are observed mostly around the Bragg peaks and near the (1.3 1.3 1.3) position (where Rowe *et al.* [11] have also obtained a peak, attributed to the ω phase).

The time-of-flight separation was not accurate enough to eliminate the low energy phonons near the Bragg peaks and a deconvolution method was developed in order to increase this accuracy [12]. A time-of-flight spectrum is shown in figure 2 with the deconvolution fit. This deconvolution method does not work very close to the Bragg positions where the distance between two peaks is small compared to their width which is nearly the same for the inelastic peaks and for the elastic one.

After this deconvolution treatment of data, the cubic symmetry of the intensity map, which is not respected by the inelastic contribution, is recovered (see fig. 1a). The difference between the intensities before and after deconvolution is given in figure 1c in the same scales as figure 1a. Only around the Bragg peaks is this difference not negligible : this is due to the low energy phonons. By comparison with figure 1a, it is clear that high diffuse intensities appear around the Bragg peaks in regions where no low-energy phonon contributions are measured so that these intensities cannot be attributed to inelastic scattering processes.

3. Interpretation.

The shape of the diffuse intensity around the Bragg peaks strongly suggests the presence of a Huang type scattering originating in the long range distortion field produced by the oxygen interstitials. The symmetry of this diffuse intensity signal is in good agreement with the isointensity contours calculated by Flocken and Hardy [13] for double-force defects ; it is thus coherent with the assumption of an octahedral site for the defect (but also with a tetrahedral one !). A further analysis is needed for this part of the signal. In the following we have restricted our interpretation to the distortions close to the defects and thus the points in a sphere of radius $R = 0.3 \times (2\,\pi/a)$ around the Bragg peaks have been eliminated for the fit.

Among the SRO peaks observed by de Novion and Just [4], in our experiment only a weak maximum is present in the (0 0 1) position with an amplitude of about 1 Laue instead of 3 Laue in [4]. The SRO intensity measured in both experiments is very weak compared to the size effect contribution. Moreover the SRO maxima positions suggest a doubling of the lattice cell and thus a heterogenous distribution of some oxygen atoms with formation of small suboxides clusters. In a first approach we have thus developed a model which neglects the interactions between impurities.

3.1 MODEL. — In principle, because of the very large distortions expected around the impurity, it is not possible to use the common development in series of the displacement term in the scattered intensity [14]. Similarly the Kanzaki forces method, which remains in the harmonic approximation, is not justified.

In the following approximations :

— the defects are isolated (not interacting),

— they occupy octahedral sites (hypothesis confirmed by proton channeling results [15]),

so that there are three possible orientations of the defects, their first neighbours being along one of the three cubic axes **a, b, c,**

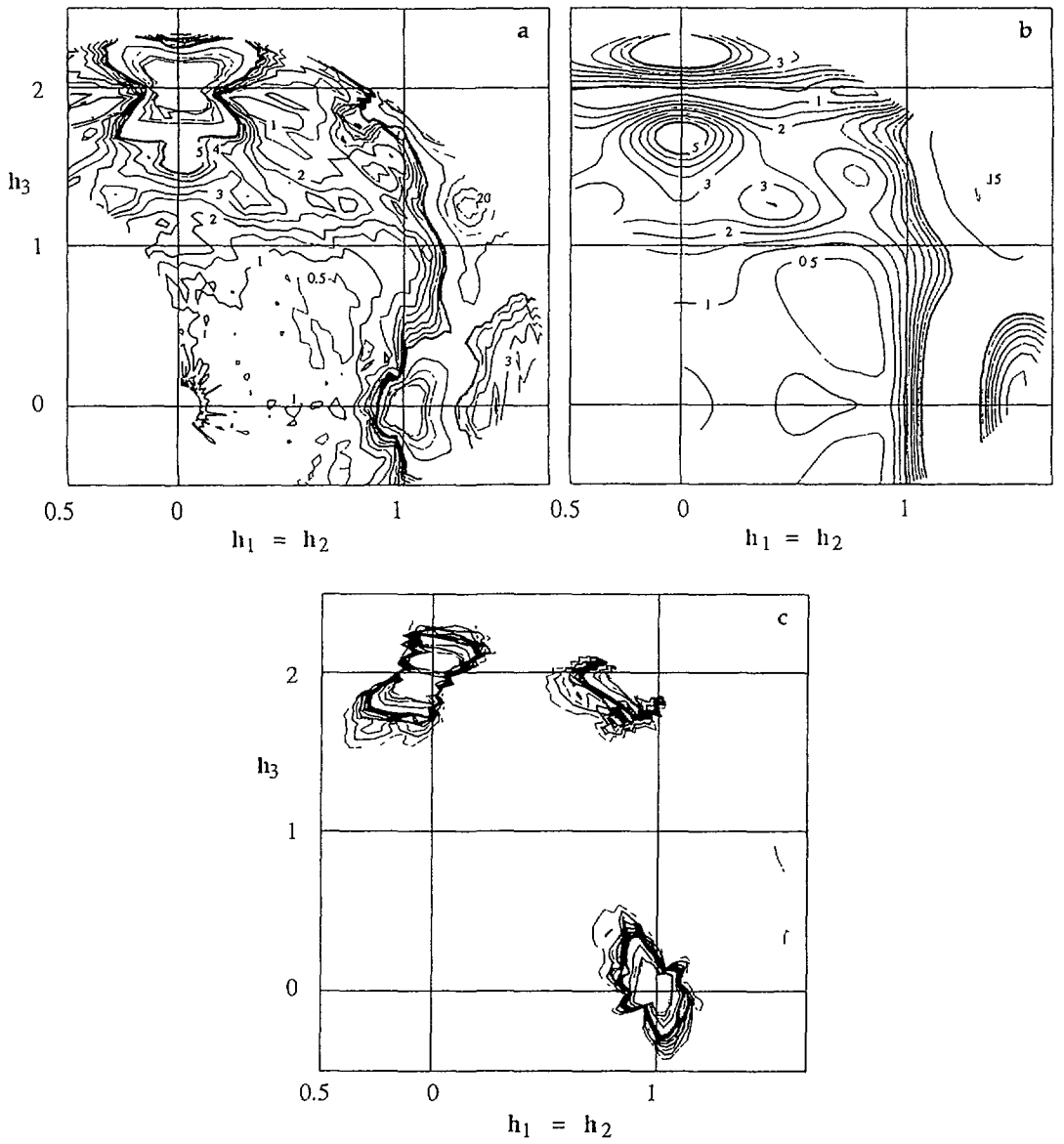

Fig. 1. — Neutron elastic diffuse intensity maps in the $\{1\bar{1}0\}$ reciprocal plane of $NbO_{0.023}$ in Laue units : iso-intensity lines from 0.5 to 5 (bold line) with a step 0.5 and from 5 to 25 with a step 5 : a) experimental map (after deconvolution), b) intensity map rebuilt from the fit parameters (in bold in Tab. I), c) difference between the intensities after the usual elastic separation and after the deconvolution treatment.

— the tetragonal symmetry of the defect site is kept,

— only three or four atomic shells around the defects are perturbed, the total intensity for the scattering vector **q** is the sum of the intensities calculated for each interstitial (averaged on the three defect orientations) :

$$I(\mathbf{q}) = \frac{1}{3} \times N \times c \times (|\mathcal{A}_a(\mathbf{q})|^2 + |\mathcal{A}_b(\mathbf{q})|^2 + |\mathcal{A}_c(\mathbf{q})|^2)$$

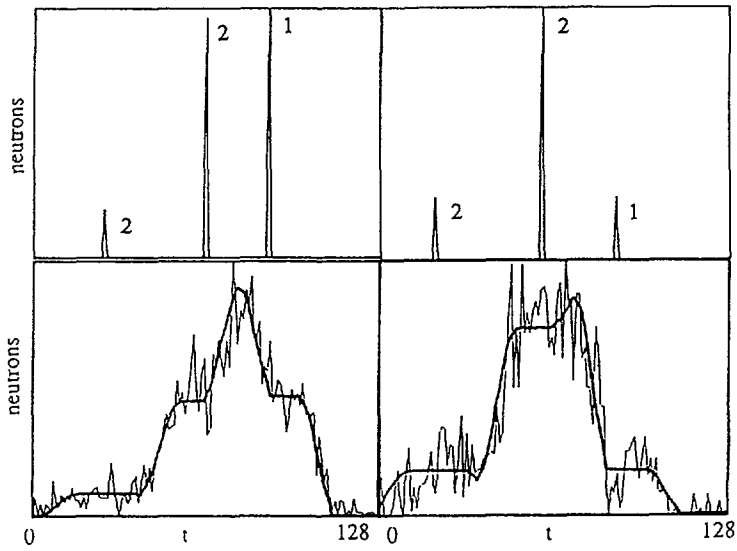

Fig. 2. — As a function of time (given in time-of-flight channel number) for two spectra : in the upper part, the ideal peaks (zero width) for elastically scattered neutrons (1), and for neutrons having interacted with a phonon (2) (their number, position and intensity are parameters of the fit) ; in the lower part the experimental spectra with the curve obtained from the above peaks broadened by the instrumental response curve (measured on the vanadium standard).

with

$$\mathcal{A}(\mathbf{q}) = b_O + \sum_{i}^{4\ \text{shells}} b_{Nb} \times \exp(i\mathbf{q} \cdot \mathbf{r}_i) + \sum_{j} b_{Nb} \times \exp(i\mathbf{q} \cdot \mathbf{R}_j) \qquad (1)$$

where N is the number of niobium sites and $N \times c$ the number of oxygen atoms, $b_O = 5.8$ fm and $b_{Nb} = 7.1$ fm [16] are the scattering lengths of oxygen and niobium atoms resp., $\mathbf{r}_i$ is the actual position of the atom i while $\mathbf{R}_i$ is the unperturbed lattice site (the origin being located on the impurity), and $\sum_j$ is the sum over all the unperturbed atoms.

The coordinates ℓmn of a lattice site i are defined by $\mathbf{R}_i = \ell \cdot \mathbf{a}/2 + m \cdot \mathbf{b}/2 + n \cdot \mathbf{c}/2$, the coordinates of the atoms are $r^\alpha(\ell mn)$ with $\alpha = x, y, z$, and the distortions $\delta r^\alpha(\ell mn) = r^\alpha(\ell mn) - R_i^\alpha$. The four first shells are $\ell mn = 100$, 011, 102 and 211. The last sum in formula (1) gives rise to a Bragg intensity, and the amplitude due to a defect oriented along **a** can be rewritten :

$$\begin{aligned}
\mathcal{A}_a(\mathbf{q}) = {} & b_O + 2\, b_{Nb}[\cos q_x r_1 + 2 \cos q_y r_2 \cos q_z r_2 \\
& + 2 \cos q_x r_3 (\cos q_y r_4 + \cos q_z r_4) \\
& + 4 \cos q_x r_5 \cos q_y r_6 \cos q_z r_6] \\
& - 2\, b_{Nb}[\cos q_x a/2 + 2 \cos q_y a/2 \cos q_z a/2 \\
& + 2 \cos q_x a/2 (\cos q_y a + \cos q_z a) \\
& + 4 \cos q_x a \cos q_y a/2 \cos q_z a/2] + \sum_{i}^{\text{all Nb sites}} b_{Nb} \times \exp(i\mathbf{q} \cdot \mathbf{R}_i)
\end{aligned}$$

with :

q_x, q_y, q_z coordinates of the scattering vector $\mathbf{q}$

$r_1 = \mathbf{r}^x(100)$, $r_2 = \mathbf{r}^y(011) = \mathbf{r}^z(011)$,

$r_3 = \mathbf{r}^x(102)$, $r_4 = \mathbf{r}^z(102)$,

$r_5 = \mathbf{r}^x(211)$, $r_6 = \mathbf{r}^y(211) = \mathbf{r}^z(211)$

(Because of the tetragonal symmetry, $\mathbf{r}^y(100) = \mathbf{r}^z(100) = \mathbf{r}^x(011) = \mathbf{r}^y(102) = 0$.)

The coordinates r_i are the parameters of a non-linear least-squares fit on the data, using the Levenberg-Marquardt algorithm [17].

3.2 RESULTS. — Several fits were tried in order to check the influence on the results of some fit conditions :

— the radius R of the sphere around Bragg peaks where data have been eliminated (as explained at the beginning of Sect. 3) was varied from 0.1 to 0.3 in $(2\pi/a)$ units,

— the perturbation range was extended from the third to the fourth atomic shell around the defect (from 14 to 22 displaced atoms).

The incoherent cross-section of our sample is not well known (see Sect. 2.2). It has been treated as a free parameter.

The results are given in table 1 together with those of Dosch *et al.* [1]. The latter are in a good agreement with the results of a lattice statics calculation by Baoping *et al.* [18] using the Green functions formalism ($\delta r^x(100) = 0.40$ Å, $\delta r^y(011) = -0.11$ Å). This is not very surprising since the two methods are based upon the same harmonic approximation.

The atomic displacements are almost insensitive to the fit conditions, and the first one is very large. These values are similar to those of Dosch *et al.* but somewhat smaller.

The intensities in figure 1b have been calculated from the parameters in bold in table I. The diffuse scattering is well reproduced except on the (1.3 1.3 1.3) maximum and near the Bragg peaks. In the latter case the scattered intensities are of Huang type, associated with the displacement field far from the defect which is not taken into account in our model, and the data are also more or less contaminated by inelastic contributions.

Table I. — *Static displacements in* Å *in* $NbO_{0.023}$ *as obtained from our model with three and with four perturbed shells around the oxygen atom and for different values of R (distance below which the data near a Bragg peak are eliminated). The values given in the right hand column are the components of the radial displacements obtained by Dosch et al.* [1] *from the Kanzaki model.*

$R/(2\pi/a)$	0.1	0.2	0.3		Dosch *et al.*
$\delta r^x(100)$	0.32	0.31	0.29	0.31	0.42
$\delta r^y(011)$	− 0.04	− 0.04	− 0.04	− 0.04	− 0.09
$\delta r^x(102)$	0.01	0.01	0.01	0.01	0.03
$\delta r^z(102)$	0.05	0.05	0.04	0.04	0.05
$\delta r^x(211)$	0.03	0.03		0.03	0.06
$\delta r^y(211)$	0.05	0.04		0.03	0.03
σ_{inc}(mb)	2.8	2.6	2.4	2.4	
χ^2	0.38	0.25	0.23	0.18	

4. Discussion.

As for interstitial C atoms occupying octahedral sites in the face centred cubic Ni [12] and as Dosch *et al.* have found for N and O in Nb [1, 2], we observe that the first shell is strongly repulsed and the second shell attracted by the interstitial.

These large distortions should influence the static Debye-Waller factor (SDWF). Indeed this SDWF has been measured in the VO_x system for several defect concentrations [19]. In VO_x as in NbO_x, lattice statics calculations have shown that the displacements of the two first neighbours of a defect in a b.c.c. octahedral site are largely dominant and in particular much stronger than those of the four second-neighbours [20]. Assuming that the SDWF is only due to these first-neighbours distortions, we obtain from [19] $\delta r^x(100) \approx 0.4$ Å for the first neighbours of an oxygen atom in vanadium ; although the small displacement approximation required for this calculation is not really justified, this $\delta r^x(100)$ value is in qualitative agreement with the lattice statics calculations of Tewary [20] in a two-forces model for VO_x(0.8 Å) and for NbO_x(0.5 Å) and with our result for NbO_x.

Dosch *et al.* have measured the diffuse scattering around some ω peak positions. They have projected the displacements of the two first shells along a (111) direction. The result is similar to what is observed in the ω phase (obtained by displacements of [111] planes towards each other). The distortions (concerning 6 niobium atoms) are thus considered as a first step to a rumpled ω phase.

In our experiment, as in the measurements of Rowe *et al.* [11], the 2/3 (111) peak of the fully collapsed ω phase is absent, and the only diffuse maximum is nearer of 5/4 (111) than of 4/3 (111), so that the explanation of the diffuse scattering by the formation of ω phase embryos is not imposed by the results (but not excluded).

On the other hand it is sure that the short range of the displacement field in our model (four shells), does not allow to explain the experimental narrow maximum : this is better done by the Kanzaki forces model. But the first atomic displacements are more reliable in our model which requires no assumption on their amplitude. It is even surprising that the harmonic approximation gives calculated intensities in such a good agreement with the experimental results in this system with distortions of 0.3 Å for the first O-Nb pair and 0.15 Å for the most distorted Nb-Nb pair. The contribution of these first pairs to the narrow peaks studied by Dosch *et al.* is probably weak.

5. Summary and conclusions.

The neutron diffuse scattering has been measured on a single crystal $NbO_{0.023}$ in the reciprocal plane $[1\bar{1}0]$. For this composition, the SRO peaks measured by de Novion and Just [4] are not observed, probably because of a more efficient quench in our case. The conditions for the appearance of this SRO, also suspected from internal friction measurements [7], are to be explored.

The diffuse intensity is interpreted with the help of a model assuming that the defects are isolated, without any assumption about the amplitude of the atomic displacements. The first neighbours of the interstitial are strongly pushed away (from 1.65 Å to 1.96 Å) and the second neighbours come slightly nearer (from 2.34 Å to 2.25 Å) : only half of the distance is done on the way to recover a regular Nb octahedron satisfying the symmetry of the oxygen p orbitals. These displacements are smaller than those deduced from a Kanzaki forces model [1] or from lattice static calculations [18], but these two methods imply the same harmonic approximation which is not justified for large distortions.

References

[1] DOSCH H. and PEISL J., *Phys. Rev. B* **21** (1985) 623.
[2] DOSCH H., v. SCHWERIN A. and PEISL J., *Phys. Rev. B* **34** (1986) 1654-1661.
[3] KANZAKI H., *J. Phys. Chem. Solids* **2** (1957) 24-36.
[4] DE NOVION C. H. and JUST W., *J. Phys. F : Met. Phys.* **8** (1978) 1627.
[5] GIBALA R. and WERT C. A., *Acta Met.* **14** (1966) 1095-1113.
[6] VILLAGRANA R. E. and THOMAS G., *Phys. Stat. Solidi* **9** (1965) 499-518.
[7] WELLER M., ZHANG J. X., SCHULZE K., KE T. S. and DIEHL J., *J. Phys. Colloq. France* **42** (1981) C5-817.
[8] FROMM E. and HORZ G., Hydrogen, nitrogen, oxygen and carbon in metals, *Int. Met. Rev.* **5-6** (1980) 269-311.
[9] CAUDRON R. and FINEL A., Rapport technique ONERA 11/1221M (1983).
[10] BAUER G., SEITZ E. and JUST W., *J. Appl. Cryst.* **8** (1975) 162-175.
[11] ROWE J. M. and MAGERL A., *Phys. Rev. B* **21** (1980) 1706-1707.
[12] BARBÉRIS P., Thèse de doctorat, Université Paris-Sud, Orsay, France (1991).
[13] FLOCKEN J. W. and HARDY J. R., *Phys. Rev. B* **1** (1970) 2472-2483.
[14] BORIE B. and SPARKS C. J., *Acta Cryst.* **A 27** (1971) 198-201.
[15] MATYASH P. P., SKAKUN N. A. and DIKII N. P., *JETP Lett.* (July 1974), translated from *Zh. Eskp. Teor. Fiz. Pis'ma* **19** (1974), 31-33.
[16] BACON G. E., Neutron Diffraction (Clarendon Press, Oxford, 1975).
[17] PRESS W. H., FLANNERY B. P., TEUKOLSKY S. A. and VETTERLING W. T., Numerical recipes in C (Cambridge University Press, 1988).
[18] BAOPING H., SATISH R. and HOUSKA C. R., *J. Mater. Sci.* **25** (1990) 2667.
[19] MCINTIRE W. R. and COHEN J. B., *Acta Met.* **23** (1975) 953-956.
[20] TEWARY V. K., *J. Phys. F* **3** (1973) 1515-1523.